

THE QUANTUM UNIVERSE*

J. AMBJØRN^{a,b}, A. GÖRLICH^c, J. JURKIEWICZ^c, R. LOLL^b^aThe Niels Bohr Institute, Copenhagen University
Blegdamsvej 17, 2100 Copenhagen, Denmark^bInstitute for Theoretical Physics, Utrecht University
Leuvenlaan 4, 3584 CE Utrecht, The Netherlands^cInstitute of Physics, Jagellonian University
Reymonta 4, 30-059 Kraków, Poland*(Received October 10, 2008)*

In this paper we review how a background independent non-perturbative regularization of quantum gravity, denoted causal dynamical triangulation (CDT), in the infrared leads to the standard minisuperspace effective action. We show how it is possible to study in detail the quantum fluctuations around the classical solution to the minisuperspace action and outline how one in principle might be able to study the quantum gravity theory in the sub-Planckian regime.

PACS numbers: 04.60.Gw, 04.60.Nc, 98.80.Qc

1. Introduction

A major unsolved problem in theoretical physics is to reconcile the classical theory of general relativity with quantum mechanics. One such attempt is string theory. However, until now it has added little to our understanding of why we, to a very good approximation, live in a 3+1 dimensional classical world governed by Einstein's equations with a positive cosmological constant, around which there presumably are small quantum fluctuations. Loop quantum gravity is another attempt to quantize gravity, introducing new ways of treating gravity at the Planck scale, but having problems with recovering classical gravity in the infrared limit. Here we report on a much more mundane approach using only standard quantum field theory. In a sum-over-histories approach we will attempt to define a nonperturbative quantum field theory which has as its infrared limit ordinary classical general relativity and at the same time has a nontrivial ultraviolet limit. From

* Presented at the XLVIII Cracow School of Theoretical Physics, "Aspects of Duality", Zakopane, Poland, June 13–22, 2008.

this point of view it is in the spirit of the renormalization group approach, first advocated long ago by Weinberg [1], and more recently substantiated by several groups of researchers [2]. However, it has some advantages compared to the renormalization group approach in that it allows us to study (numerically) certain geometric observables which are difficult to handle analytically.

We define the path integral of quantum gravity nonperturbatively using the lattice approach known as *causal dynamical triangulations* (CDT) as a regularization. CDT establishes a nonperturbative way of performing the sum over four-geometries (for more extensive definitions, see [4, 5]). It sums over the class of piecewise linear four-geometries which can be assembled from four-dimensional simplicial building blocks of link length a , such that only *causal* spacetime histories are included.

The challenge when searching for a *field theory* of quantum gravity is three-fold: (i) to find a suitable nonperturbative formulation of such a theory which satisfies a minimum of reasonable requirements, like background independence, and the emergence of a semiclassical four-dimensional geometry, (ii) to find *observables* which can be used to test that the lattice theory has a continuum limit when the UV cut-off (the inverse lattice spacing) is taken to infinity, and (iii) to actually show that one can adjust the bare coupling constants of the regularized theory such that a continuum limit is reached. Although we will focus on (i) in what follows, let us immediately mention that (ii) is notoriously difficult in a theory of quantum gravity, where one is faced with a number of questions originating in the dynamical nature of geometry. What is the meaning of distance when integrating over all geometries? How do we attach a meaning to local spacetime points like x and y if we want to discuss a propagator $\langle \phi(x)\phi(y) \rangle$ of some field ϕ ? How can we define at all local, diffeomorphism-invariant quantities in the continuum which can then be translated to the regularized (lattice) theory? — What we want to point out here is that although (i)–(iii) are standard requirements when relating critical phenomena and (Euclidean) quantum field theory, gravity *is* special and may require a reformulation of (part of) the standard scenario of defining nonperturbatively a lattice field theory and then taking the continuum limit.

Our proposed nonperturbative formulation of four-dimensional quantum gravity has a number of nice features. First, it sums over a class of piecewise linear geometries. Piecewise linear geometries have the nice feature that the one does not need to introduce coordinate systems to obtain a complete description of the geometry. In this way we perform the sum over geometries directly, avoiding the cumbersome procedure of first introducing a coordinate system and then getting rid of the ensuing gauge redundancy, as one has to do in a continuum calculation. Our underlying assumptions are that the

class of piecewise linear geometries is in a suitable sense dense in the set of all geometries relevant for the path integral (probably a fairly mild assumption), and that we are using a correct measure on the set of geometries. This is a more questionable assumption since we do not even know whether such a measure exists. Here one has to take a pragmatic attitude in order to make progress. We will simply examine the outcome of our construction and try to judge whether it is promising.

Secondly, our scheme is background-independent. No distinguished geometry, accompanied by quantum fluctuations, is put in by hand. If the CDT-regularized theory is to be taken seriously as a potential theory of quantum gravity, there has to be a region in the space spanned by the bare coupling constants where the geometry of spacetime bears some resemblance with the kind of universe we observe around us. That is, the theory should create dynamically an effective background geometry around which there are (small) quantum fluctuations. This is a very nontrivial property of the theory and we will show that such a picture emerges from the computer simulations [3, 7–9]. They establish the de Sitter nature of the background spacetime, quantify the fluctuations around it, and set a physical scale for the universes we are dealing with.

2. The CDT formalism

The lattice formulation of Euclidean quantum gravity, *i.e.* the quantum theory of Euclidean geometries, has been very successful in two dimensions. In two dimensions there is not a dynamical quantum gravity theory, but two-dimensional Euclidean quantum gravity is a diffeomorphism invariant quantum theory of geometries. The lattice theory, regularized by the method of so-called dynamical triangulations (DT), provides a diffeomorphism invariant cut-off of two-dimensional Euclidean quantum gravity. Thus it is a misconception that a lattice regularization will necessarily break diffeomorphism invariance. Rather one should view the use of DT in the path integral as a way to sum directly over *geometries*, thus avoiding completely the issue of diffeomorphism invariance. The reason such an interpretation is possible is, as mentioned above, that the triangulations used in DT can be viewed as piecewise linear geometries without any specific metric assigned to them: once we know the length of the links and the gluing of the simplices we have complete information about the geometry. Using identical simplices the basic information about the geometry is entirely encoded in the way the simplices are glued together and the summation over geometries becomes the summation over possible abstract triangulations. The UV cut-off is the length a of the sides of the simplices. Using the formalism one can formulate an Euclidean theory of quantum gravity using as building

blocks Euclidean equilateral simplices and using two-dimensional building blocks (triangle) one obtains a lattice version of two-dimensional quantum gravity. It can be solved analytically for finite a and agrees with a continuum quantization of two-dimensional *Euclidean* gravity (quantum Liouville theory) in the limit $a \rightarrow 0$. However, in higher dimensions this Euclidean lattice approach seemed not to have the desired continuum limit. This was one motivation to introduce a modified approach based on so-called causal dynamical triangulations (CDT).

CDT stands in the tradition of [12], which advocated that in a gravitational path integral with the correct, Lorentzian signature of spacetime one should sum over causal geometries only. More specifically, we adopted this idea when it became clear that attempts to formulate a *Euclidean* nonperturbative quantum gravity theory run into trouble in spacetime dimension d larger than two.

This implies that we start from Lorentzian simplicial space-times with $d = 4$ and insist that only causally well-behaved geometries appear in the (regularized) Lorentzian path integral. A crucial property of our explicit construction is that each of the configurations allows for a rotation to Euclidean signature. We rotate to a Euclidean regime in order to perform the sum over geometries (and rotate back again afterward if needed). We stress here that although the sum is performed over geometries with Euclidean signature, it is different from what one would obtain in a theory of quantum gravity based ab initio on Euclidean space-times. The reason is that not all Euclidean geometries with a given topology are included in the “causal” sum since in general they have no correspondence to a causal Lorentzian geometry.

We refer to [4] for a detailed description of how to construct the class of piecewise linear geometries used in the Lorentzian path integral. The most important assumption is the existence of a global proper-time foliation. This is symbolically illustrated in Fig. 1 where we compare the construction to the

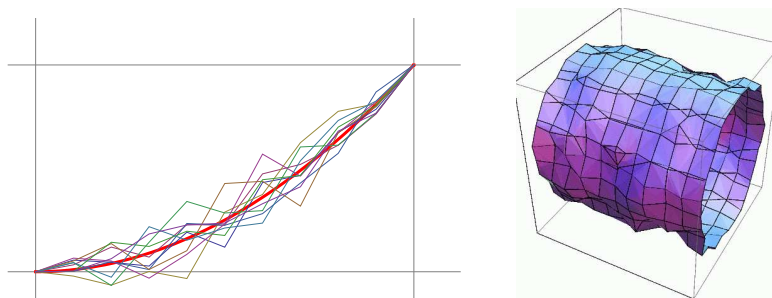


Fig. 1. Piecewise linear space-time histories in quantum mechanics and in 1+1 dimensional quantum gravity.

one of ordinary quantum mechanics: the path integral of ordinary quantum mechanics is regularized as a sum over piecewise linear paths from point x to point y in time t , the continuum limit being obtained when the lengths of these “building blocks” go to zero. Similarly, in the quantum gravity case we have a sum over four-geometries, “stretching” between two three-geometries separated a proper time t and constructed from four-dimensional building blocks, as described below. On the figure we have for obvious illustrative reasons replaced the three-dimensional spatial geometries with one-dimensional spatial geometries with the topology of S^1 .

We assume that the spacetime topology is that of $S^3 \times R$, the spatial topology being that of S^3 merely by convenience. The spatial geometry at each discrete proper-time step t_n is represented by a triangulation of S^3 , made up of equilateral spatial tetrahedra with squared side-length $\ell_s^2 \equiv a^2 > 0$. In general, the number $N_3(t_n)$ of tetrahedra and how they are glued together to form a piecewise flat three-dimensional manifold will vary with each time-step t_n . In order to obtain a four-dimensional triangulation, the individual three-dimensional slices must still be connected in a causal way, preserving the S^3 -topology at all intermediate times t between t_n and t_{n+1} ¹. This is done as illustrated in Fig. 2, introducing what we call (4,1)-simplices and (3,2)-simplices. In the path integral we will be summing over all possible ways to connect a given 3d triangulation at time t_n and a given 3d triangulation at t_{n+1} to a slab of 4d space-time as shown in Fig. 2, and in addition we will sum over all 3d triangulations of S^3 at times t_n .

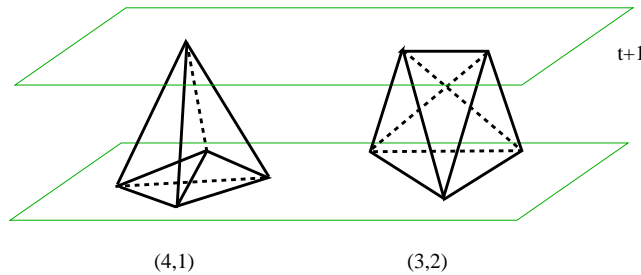


Fig. 2. (4,1) and a (3,2) simplices connecting two neighboring spatial slices. We also have symmetric (1,4) and (2,3) simplices with a vertex and a line, respectively, at time t and a tetrahedron and a triangle, respectively, at time $t+1$. For simplicity we denote the total number of (4,1) and (1,4) simplices by $N_4^{(4,1)}$ and similarly the total number of (3,2) and (2,3) simplices by $N_4^{(3,2)}$.

¹ This implies the absence of branching of the spatial universe into several disconnected pieces, so-called *baby universes*, which (in Lorentzian signature) would inevitably be associated with causality violations in the form of degeneracies in the light cone structure, as has been discussed elsewhere (see, for example, [11]).

We allow for an asymmetry between time and space lattice length assignments: Denote by ℓ_t and ℓ_s the length of the time-like links and the space-like links, respectively. Then $\ell_t^2 = -\alpha\ell_s^2$, $\alpha > 0$. The explicit rotation to Euclidean signature is done by performing the rotation $\alpha \rightarrow -\alpha$ in the complex lower half-plane, $|\alpha| > 7/12$, such that we have $\ell_t^2 = |\alpha|\ell_s^2$ (see [4] for a discussion).

The Einstein–Hilbert action S^{EH} has a natural geometric implementation on piecewise linear geometries in the form of the Regge action. This is given by the sum of the so-called deficit angles around the two-dimensional “hinges” (subsimpllices in the form of triangles), each multiplied with the volume of the corresponding hinge. In view of the fact that we are dealing with piecewise linear, and not smooth metrics, there is no unique “approximation” to the usual Einstein–Hilbert action, and one could in principle work with a different form of the gravitational action. We will stick with the Regge action, which takes on a very simple form in our case, where the piecewise linear manifold is constructed from just two different types of building blocks. After rotation to Euclidean signature one obtains for the action (see [5] for details)

$$\begin{aligned} S_{\text{E}}^{\text{EH}} &= \frac{1}{16\pi^2 G} \int d^4x \sqrt{g} (-R + 2\Lambda) \quad \longrightarrow \\ S_{\text{E}}^{\text{Regge}} &= -(\kappa_0 + 6\Delta)N_0 + \kappa_4 \left(N_4^{(4,1)} + N_4^{(3,2)} \right) + \Delta \left(2N_4^{(4,1)} + N_4^{(3,2)} \right), \end{aligned} \quad (1)$$

where N_0 denotes the total number of vertices in the four-dimensional triangulation and $N_4^{(4,1)}$ and $N_4^{(3,2)}$ denote the total number of the four-simplices described above, so that the total number N_4 of four-simplices is $N_4 = N_4^{(4,1)} + N_4^{(3,2)}$. The dimensionless coupling constants κ_0 and κ_4 are related to the bare gravitational and bare cosmological coupling constants, with appropriate powers of the lattice spacing a already absorbed into κ_0 and κ_4 . The *asymmetry parameter* Δ is related to the parameter α introduced above, which describes the relative scale between the (squared) lengths of space- and time-like links. It is both convenient and natural to keep track of this parameter in our set-up, which from the outset is not isotropic in time and space directions, see again [5] for a detailed discussion. Since we will in the following work with the path integral after Wick rotation, let us redefine $\tilde{\alpha} := -\alpha$ [5], which is positive in the Euclidean domain². For future reference, the Euclidean four-volume of our universe for a given choice of $\tilde{\alpha}$ is given by

$$V_4 = \tilde{C}_4(\xi) a^4 N_4^{(4,1)} = \tilde{C}_4(\xi) a^4 N_4 / (1 + \xi), \quad (2)$$

² The most symmetric choice is $\tilde{\alpha} = 1$, corresponding to vanishing asymmetry, $\Delta = 0$.

where ξ is the ratio

$$\xi = N_4^{(3,2)} / N_4^{(4,1)}, \tag{3}$$

and $\tilde{C}_4(\xi) a^4$ is a measure of the “effective four-volume” of an “average” four-simplex. ξ will depend on the choice of coupling constants in a rather complicated way (for a detailed discussion we refer to [3, 4]).

The path integral or partition function for the CDT version of quantum gravity is now

$$Z(G, \Lambda) = \int \mathcal{D}[g] e^{-S_E^{\text{EH}}[g]} \quad \rightarrow \quad Z(\kappa_0, \kappa_4, \Delta) = \sum_{\mathcal{T}} \frac{1}{C_{\mathcal{T}}} e^{-S_E(\mathcal{T})}, \tag{4}$$

where the summation is over all causal triangulations \mathcal{T} of the kind described above, and we have dropped the superscript “Regge” on the discretized action. The factor $1/C_{\mathcal{T}}$ is a symmetry factor, given by the order of the automorphism group of the triangulation \mathcal{T} . The actual set-up for the simulations is as follows. We choose a fixed number N of spatial slices at proper times $t_1, t_2 = t_1 + a_t$, up to $t_N = t_1 + (N-1)a_t$, where $\Delta t \equiv a_t$ is the discrete lattice spacing in temporal direction and $T = Na_t$ the total extension of the universe in proper time. For convenience we identify t_{N+1} with t_1 , in this way imposing the topology $S^1 \times S^3$ rather than $I \times S^3$. This choice does not affect physical results, as will become clear in due course.

Our next task is to *evaluate* the nonperturbative sum in (4), if possible, analytically. Although this can be done in spacetime dimension $d = 2$ ([6], and see [13] for recent developments) and at least partially in $d = 3$ [14, 15], an analytic solution in four dimensions is currently out of reach. However, we are in the fortunate situation that $Z(\kappa_0, \kappa_4, \Delta)$ can be studied quantitatively with the help of Monte Carlo simulations. The type of algorithm needed to update the piecewise linear geometries has been around for a while, starting from the use of dynamical triangulations in bosonic string theory (two-dimensional Euclidean triangulations) [16–18] and was later extended to their application in Euclidean four-dimensional quantum gravity [19, 20]. In [4] the algorithm was modified to accommodate the geometries of the CDT set-up. Note that the algorithm is such that it takes the symmetry factor $C_{\mathcal{T}}$ into account automatically.

We have performed extensive Monte Carlo simulations of the partition function Z for a number of values of the bare coupling constants. As reported in [5], there are regions of the coupling constant space which do not appear relevant for continuum physics in that they seem to suffer from problems similar to the ones found earlier in *Euclidean* quantum gravity constructed in terms of dynamical triangulations, which essentially led to its abandonment in $d > 2$. Namely, when the (inverse, bare) gravitational coupling κ_0 is sufficiently large, the Monte Carlo simulations exhibit a sequence in time

direction of small, disconnected universes, none of them showing any sign of the scaling one would expect from a macroscopic universe. We denote this phase A. We believe that this phase of the system is a Lorentzian version of the branched polymer phase of Euclidean quantum gravity. By contrast, when Δ is sufficiently small the simulations reveal a universe with a vanishing temporal extension of only a few lattice spacings, ending both in past and future in a vertex of very high order, connected to a large fraction of all vertices. This phase is most likely related to the so-called crumpled phase of Euclidean quantum gravity. We denote this phase B. The crucial and new feature of the quantum superposition in terms of *causal* dynamical triangulations is the appearance of a region in coupling constant space which is different and interesting and where continuum physics may emerge. It is in this region that we have performed the simulations discussed here and where previous work has already uncovered a number of intriguing physical results [5, 7, 8, 21]. In Fig. 4 we have shown how different configurations look in the three phases discussed above, and in Fig. 3 we have shown the tentative phase diagram in the coupling constant space $\kappa_0, \kappa_4, \Delta$.

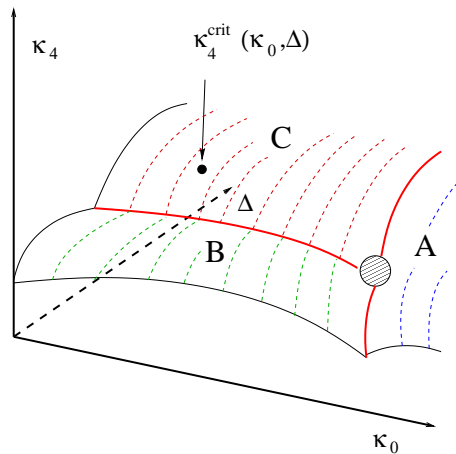


Fig. 3. The phases A, B and C in the coupling constant space $(\kappa_0, \Delta, \kappa_4)$. Phase C is the one where extended four-dimensional geometries emerge.

A “critical” surface is shown in the figure. Keep κ_0 and Δ fixed. Then κ_4 acts as a chemical potential for N_4 and the smaller κ_4 the larger $\langle N_4 \rangle$. At some critical value $\kappa_4(\kappa_0, \Delta)$, depending on the choice of κ_0 and Δ , $\langle N_4 \rangle \rightarrow \infty$. For $\kappa_4 < \kappa_4(\kappa_0, \Delta)$ the partition function is plainly divergent and not defined. When we talk about phase transitions we are always at the “critical” surface

$$\kappa_4 = \kappa_4(\kappa_0, \Delta), \quad (5)$$

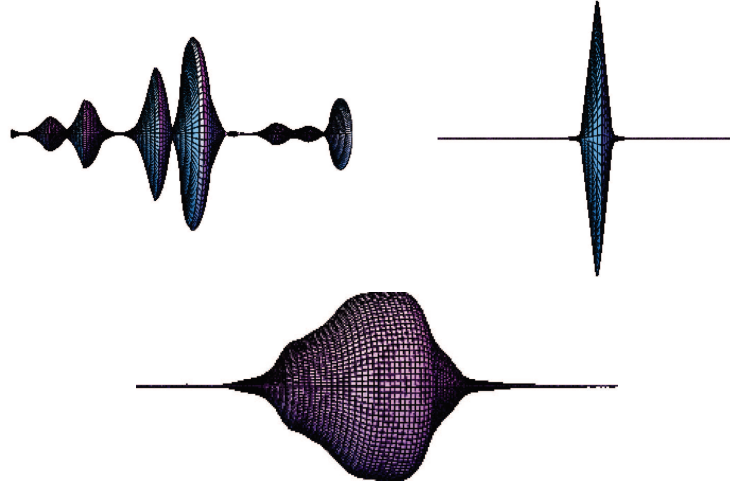


Fig. 4. Typical configurations in the phases A, B and C (lowest figure). Phase C is the one where extended four-dimensional geometries emerge.

simply because we cannot have a phase transition unless $N_4 = \infty$. We put “critical” into quotation marks since it only means that we probe infinite four-volume. No continuum limit is necessarily associated with a point on this surface. To decide this issue requires additional investigation. A good analogy is the Ising model on a finite lattice. To have a genuine phase transition for the Ising model we have to take the lattice volume to infinity since there are no genuine phase transitions for finite systems. However, just taking the lattice volume to infinity is not sufficient to ensure critical behavior of the Ising model. We also have to tune the coupling constant to its critical value. Being on the “critical” surface, or rather “infinite volume” surface (5), we can discuss various phases, and these are the ones indicated at the figure. The different phases are separated by a phase transitions which might be first order phase transition. However we have not yet conducted a systematic investigation of the order of the transitions. Looking at Fig. 3 we have two lines of phase transitions, separating phase A and phase C and separating phase B and phase C, respectively. They meet in the point indicated on the figure. It is tempting to speculate that this point be associated with a higher order transition, as is common for statistical systems in such a situation. We will return to this later.

In the Euclideanized setting the value of the cosmological constant determines the spacetime volume V_4 since the two appear in the action as conjugate variables. We therefore have $\langle V_4 \rangle \sim G/\Lambda$ in a continuum notation, where G is the gravitational coupling constant and Λ the cosmological

constant. In the computer simulations it is more convenient to keep the four-volume fixed or partially fixed. We will implement this by fixing the total number of four-simplices of type $N_4^{(4,1)}$ or, equivalently, the total number N_3 of tetrahedra making up the spatial S^3 triangulations at times t_i , $i = 1, \dots, N$,

$$N_3 = \sum_{i=1}^N N_3(t_i) = \frac{1}{2} N_4^{(4,1)}. \quad (6)$$

We know from the simulations that in the phase of interest $\langle N_4^{(4,1)} \rangle \propto \langle N_4^{(3,2)} \rangle$ as the total volume is varied [5]. This effectively implies that we only have two bare coupling constants κ_0, Δ in (4), while we compensate by hand for the coupling constant κ_4 by studying the partition function $Z(\kappa_0, \Delta; N_4^{(4,1)})$ for various $N_4^{(4,1)}$. To keep track of the ratio $\xi(\kappa_0, \Delta)$ between the expectation value $\langle N_4^{(3,2)} \rangle$ and $N_4^{(4,1)}$, which depends weakly on the coupling constants, we write (*c.f.* Eq. (3))

$$\langle N_4 \rangle = N_4^{(4,1)} + \langle N_4^{(3,2)} \rangle = N_4^{(4,1)} (1 + \xi(\kappa_0, \Delta)). \quad (7)$$

For all practical purposes we can regard N_4 in a Monte Carlo simulation as fixed. The relation between the partition function we use and the partition function with variable four-volume is given by the Laplace transformation

$$Z(\kappa_0, \kappa_4, \Delta) = \int_0^\infty dN_4 e^{-\kappa_4 N_4} Z(\kappa_0, N_4, \Delta), \quad (8)$$

where strictly speaking the integration over N_4 should be replaced by a summation over the discrete values N_4 can take. Returning to Fig. 3, keeping N_4 fixed rather than fine-tuning κ_4 to the critical value κ_4^c implies that one is already on the “critical” surface drawn in Fig. 3, assuming that N_4 is sufficiently large (in principle infinite). Whether N_4 is sufficiently large to qualify as “infinite” can be investigated by performing the computer simulations for different N_4 s and comparing the results. This is a technique we will use over and over again in the following.

3. The macroscopic de Sitter universe

The Monte Carlo simulations referred to above will generate a sequence of spacetime histories. An individual spacetime history is not an observable, in the same way as a path $x(t)$ of a particle in the quantum-mechanical path integral is not. However, it is perfectly legitimate to talk about the *expectation value* $\langle x(t) \rangle$ as well as the *fluctuations around* $\langle x(t) \rangle$. Both of these quantities are in principle calculable in quantum mechanics.

Obviously, there are many more dynamical variables in quantum gravity than there are in the particle case. We can still imitate the quantum-mechanical situation by picking out a particular one, for example, the spatial three-volume $V_3(t)$ at proper time t . We can measure both its expectation value $\langle V_3(t) \rangle$ as well as fluctuations around it. The former gives us information about the large-scale “shape” of the universe we have created in the computer. In this section, we will describe the measurements of $\langle V_3(t) \rangle$, keeping a more detailed discussion of the fluctuations to Sec. 5 below.

A “measurement” of $V_3(t)$ consists of a table $N_3(i)$, where $i = 1, \dots, N$ denotes the number of time-slices. Recall from Sec. 2 that the sum over slices $\sum_{i=1}^N N_3(i)$ is kept constant. The time axis has a total length of N time steps, where $N = 80$ in the actual simulations, and we have cyclically identified time-slice $N + 1$ with time-slice 1.

What we observe in the simulations is that for the range of discrete volumes N_4 under study the universe does *not* extend (*i.e.* has appreciable three-volume) over the entire time axis, but rather is localized in a region much shorter than 80 time slices. Outside this region the spatial extension $N_3(i)$ will be minimal, consisting of the minimal number (five) of tetrahedra needed to form a three-sphere S^3 , plus occasionally a few more tetrahedra³. This thin “stalk” therefore carries little four-volume and in a given simulation we can for most practical purposes consider the total four-volume of the remainder, the extended universe, as fixed.

In order to perform a meaningful average over geometries which explicitly refers to the extended part of the universe, we have to remove the translational zero mode which is present. We refer to [3] for a discussion of the procedure, but having defined the centre of volume along the time-direction of our spacetime configurations we can now perform superpositions of configurations and define the average $\langle N_3(i) \rangle$ as a function of the discrete time i . The results of measuring the average discrete spatial size of the universe at various discrete times i are illustrated in Fig. 5 and can be succinctly summarized by the formula

$$N_3^{\text{cl}}(i) := \langle N_3(i) \rangle = \frac{N_4}{2(1 + \xi)} \frac{3}{4} \frac{1}{s_0 N_4^{1/4}} \cos^3 \left(\frac{i}{s_0 N_4^{1/4}} \right), \quad s_0 \approx 0.59, \quad (9)$$

where $N_3(i)$ denotes the number of three-simplices in the spatial slice at discretized time i and N_4 the total number of four-simplices in the entire universe. Since we are keeping $N_4^{(4,1)}$ fixed in the simulations and since ξ

³ This kinematic constraint ensures that the triangulation remains a *simplicial manifold* in which, for example, two d -simplices are not allowed to have more than one $(d - 1)$ -simplex in common.

changes with the choice of bare coupling constants, it is sometimes convenient to rewrite (9) as

$$N_3^{\text{cl}}(i) = \frac{1}{2} N_4^{(4,1)} \frac{3}{4} \frac{1}{\tilde{s}_0 (N_4^{(4,1)})^{1/4}} \cos^3 \left(\frac{i}{\tilde{s}_0 (N_4^{(4,1)})^{1/4}} \right), \quad (10)$$

where \tilde{s}_0 is defined by $\tilde{s}_0 (N_4^{(4,1)})^{1/4} = s_0 N_4^{1/4}$. Of course, formula (9) is only valid in the extended part of the universe where the spatial three-volumes are larger than the minimal cut-off size.

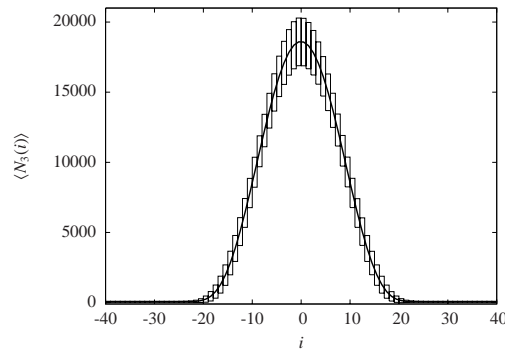


Fig. 5. Background geometry $\langle N_3(i) \rangle$: MC measurements for fixed $N_4^{(4,1)} = 160.000$ ($N_4 = 362.000$) and best fit (9) yield indistinguishable curves at given plot resolution. The bars indicate the average size of quantum fluctuations.

The data shown in Fig. 5 have been collected at the particular values $(\kappa_0, \Delta) = (2.2, 0.6)$ of the bare coupling constants and for $N_4 = 362.000$ (corresponding to $N_4^{(4,1)} = 160.000$). For this value of (κ_0, Δ) we have verified relation (9) for N_4 ranging from 45.500 to 362.000 building blocks (45.500, 91.000, 181.000 and 362.000). After rescaling the time and volume variables by suitable powers of N_4 according to relation (9), and plotting them in the same way as in Fig. 5, one finds almost total agreement between the curves for different spacetime volumes. This is illustrated in Fig. 6. Thus we have here a beautiful example of finite size scaling, and at least when we discuss the average three-volume $V_3(t)$ all our discretized volumes N_4 are large enough that we can treat them as infinite in the sense that no further change will occur for larger N_4 .

By contrast, the quantum fluctuations indicated in Fig. 5 as vertical bars *are* volume-dependent and will be the larger the smaller the total four-volume, see Sec. 5 below for details Eq. (9) shows that spatial volumes

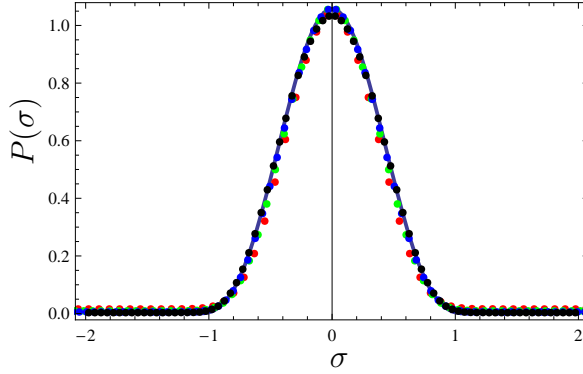


Fig. 6. Rescaling of time and volume variables according to relation (9) for $N_4 = 45.500, 91.000, 181.000$ and 362.000 . The plot also include the curve (9). More precisely: $\sigma \propto i/N_4^{1/4}$ and $P(\sigma) \propto N_3(i)/N_4^{3/4}$.

scale according to $N_4^{3/4}$ and time intervals according to $N_4^{1/4}$, as one would expect for a genuinely *four*-dimensional spacetime and this is exactly the scaling we have used in Fig. 6. This strongly suggests a translation of (9) to a continuum notation. The most natural identification is given by

$$\sqrt{g_{tt}} V_3^{\text{cl}}(t) = V_4 \frac{3}{4B} \cos^3 \left(\frac{t}{B} \right), \tag{11}$$

where we have made the identifications

$$\frac{t_i}{B} = \frac{i}{s_0 N_4^{1/4}}, \quad \Delta t_i \sqrt{g_{tt}} V_3(t_i) = 2\tilde{C}_4 N_3(i) a^4, \tag{12}$$

such that we have

$$\int dt \sqrt{g_{tt}} V_3(t) = V_4. \tag{13}$$

In (12), $\sqrt{g_{tt}}$ is the constant proportionality factor between the time t and genuine continuum proper time τ , $\tau = \sqrt{g_{tt}} t$. (The combination $\Delta t_i \sqrt{g_{tt}} V_3$ contains \tilde{C}_4 , related to the four-volume of a four-simplex rather than the three-volume corresponding to a tetrahedron because its time integral must equal V_4). Writing $V_4 = 8\pi^2 R^4/3$, and $\sqrt{g_{tt}} = R/B$, Eq. (11) is seen to describe a Euclidean *de Sitter universe* (a four-sphere, the maximally symmetric space for positive cosmological constant) as our searched-for, dynamically generated background geometry! In the parametrization of (11) this is the classical solution to the action

$$S = \frac{1}{24\pi G} \int dt \sqrt{g_{tt}} \left(\frac{g^{tt} \dot{V}_3^2(t)}{V_3(t)} + k_2 V_3^{1/3}(t) - \lambda V_3(t) \right), \tag{14}$$

where $k_2 = 9(2\pi^2)^{2/3}$ and λ is a Lagrange multiplier, fixed by requiring that the total four-volume be V_4 , $\int dt \sqrt{g_{tt}} V_3(t) = V_4$. Up to an overall sign, this is precisely the Einstein–Hilbert action for the scale factor $a(t)$ of a homogeneous, isotropic universe (rewritten in terms of the spatial three-volume $V_3(t) = 2\pi^2 a(t)^3$), although we, of course, never put any such simplifying symmetry assumptions into the CDT model.

A discretized, dimensionless version of (14) is

$$S_{\text{discr}} = k_1 \sum_i \left(\frac{(N_3(i+1) - N_3(i))^2}{N_3(i)} + \tilde{k}_2 N_3^{1/3}(i) \right), \quad (15)$$

where $\tilde{k}_2 \propto k_2$. This can be seen by applying the scaling (9), namely, $N_3(i) = N_4^{3/4} n_3(s_i)$ and $s_i = i/N_4^{1/4}$. This enables us to finally conclude that the identifications (12) when used in the action (15) lead naïvely to the continuum expression (14) under the identification

$$G = \frac{a^2 \sqrt{\tilde{C}_4} \tilde{s}_0^2}{k_1 3\sqrt{6}}. \quad (16)$$

Next, let us comment on the universality of these results. First, we have checked that they are not dependent on the particular definition of time-slicing we have been using, in the following sense. By construction of the piecewise linear CDT-geometries we have at each integer time step $t_i = i a_t$ a spatial surface consisting of $N_3(i)$ tetrahedra. Alternatively, one can choose as reference slices for the measurements of the spatial volume non-integer values of time, for example, all time slices at discrete times $i - 1/2$, $i = 1, 2, \dots$. In this case the “triangulation” of the spatial three-spheres consists of tetrahedra — from cutting a (4,1)- or a (1,4)-simplex half-way — and “boxes”, obtained by cutting a (2,3)- or (3,2)-simplex (the geometry of this is worked out in [22]). We again find a relation like (9) if we use the total number of spatial building blocks in the intermediate slices (tetrahedra+boxes) instead of just the tetrahedra.

Second, we have repeated the measurements for other values of the bare coupling constants. As long as we stay in the phase where an extended universe is observed, the phase C in Fig. 3, a relation like (9) remains valid. In addition, the value of s_0 , defined in Eq. (9), is almost unchanged until we get close to the phase transition lines beyond which the extended universe disappears. Fig. 7 shows the average shape $\langle N_3(t) \rangle$ for $\Delta = 0.6$ and for κ_0 equal to 2.2 and 3.6. Only for the values of κ_0 around 3.6 and larger will the measured $\langle N_3(t) \rangle$ differ significantly from the value at 2.2. For values larger than 3.8 (at $\Delta = 0.6$), the universe will disintegrate into a number of small and disconnected components distributed randomly along the time axis, and

one can no longer fit the distribution $\langle N_3(t) \rangle$ to the formula (9). Fig. 8 shows the average shape $\langle N_3(t) \rangle$ for $\kappa_0 = 2.2$ and Δ equal to 0.2 and 0.6. Here the value $\Delta = 0.2$ is close to the phase transition where the extended universe will flatten out to a universe with a time extension of a few lattice spacings only. Later we will show that while s_0 is almost unchanged, the constant k_1 in (15), which governs the quantum fluctuations around the mean value $\langle N_3(t) \rangle$, is more sensitive to a change of the bare coupling constants, in particular in the case where we change κ_0 (while leaving Δ fixed).

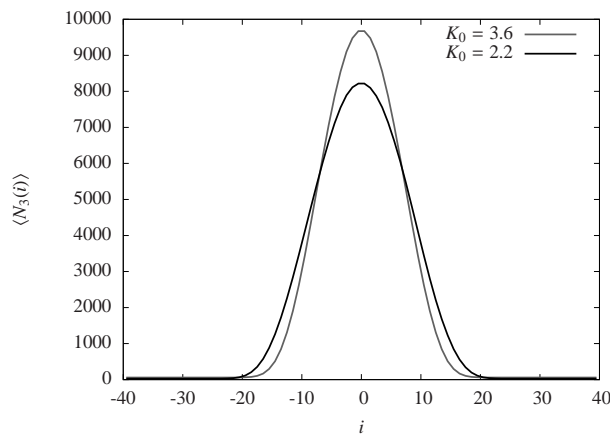


Fig. 7. The measured average shape $\langle N_3(i) \rangle$ of the quantum universe at $\Delta = 0.6$, for $\kappa_0 = 2.2$ (broader distribution) and $\kappa_0 = 3.6$ (narrower distribution), taken at $N_4^{(4,1)} = 160.000$.

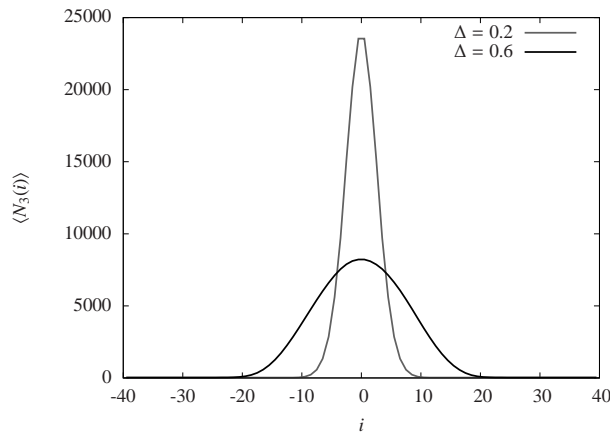


Fig. 8. The measured average shape $\langle N_3(i) \rangle$ of the quantum universe at $\kappa_0 = 2.2$, for $\Delta = 0.6$ (broad distribution) and $\Delta = 0.2$ (narrow distribution), both taken at $N_4^{(4,1)} = 160.000$.

4. Constructive evidence for the effective action

We have found a perfect fit (9) to the emergent background geometry and the curve can be understood from the continuum effective action (14). It is, however, still of interest to investigate to which extent the data will lead us to the action (15).

We have the following data: (1) the measurement of $N_3(i)$, that is, the three-volume at the discrete time step i , and the measurement of the three-volume correlator $N_3(i)N_3(j)$. Having created K statistically independent configurations $N_3^{(k)}(i)$ by Monte Carlo simulation allows us to construct the average

$$\bar{N}_3(i) := \langle N_3(i) \rangle \cong \frac{1}{K} \sum_k N_3^{(k)}(i), \quad (17)$$

where the superscript in $(\cdot)^{(k)}$ denotes the result of the k -th configuration sampled. (2) the covariance matrix

$$C(i, j) \cong \frac{1}{K} \sum_k \left(N_3^{(k)}(i) - \bar{N}_3(i) \right) \left(N_3^{(k)}(j) - \bar{N}_3(j) \right). \quad (18)$$

We now assume we have a discretized action which can be expanded around the expectation value $\bar{N}_3(i)$ according to

$$S_{\text{discr}}[\bar{N} + n] = S_{\text{discr}}[\bar{N}] + \frac{1}{2} \sum_{i,j} n_i \hat{P}_{ij} n_j + O(n^3). \quad (19)$$

If the quadratic approximation describes the quantum fluctuations around the expectation value \bar{N} well, the inverse of \hat{P} will be a good approximation to the covariance matrix. Conversely, still assuming the quadratic approximation gives a good description of the fluctuations, the \hat{P} constructed from the covariance matrix will to a good approximation allow us to reconstruct the action via (19).

Fig. 9 shows the measured covariance matrix $C(i, j)$ and its inverse, which in the approximation mentioned above can be viewed as a “propagator” \hat{P} . Some care is needed to invert $C(i, j)$ since it has two zero modes: one from the constraint that N_4 is kept fixed and (an approximate) one from the fact that the translational mode of the “center” of mass can only be fixed up to a lattice spacing, (for a detailed discussion we refer to [3]). As is clear from the figure \hat{P} is entirely dominated by the stalk data. This is of course unfortunate but unavoidable: while the correlation matrix is dominated by the long range fluctuations, the inverse matrix will be dominated by the short distance fluctuations, *i.e.* the fluctuations in the stalk which is, by definition of the stalk, of cut-off energies.

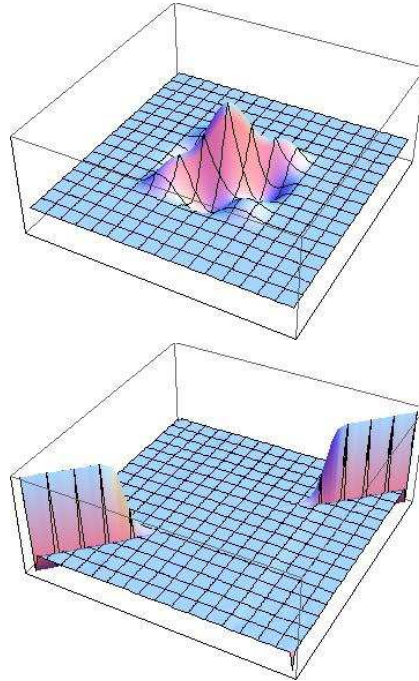


Fig. 9. The propagator and its inverse.

Looking at the inverse \hat{P} of the measured covariance matrix, we observe that it is to a very good approximation small and constant except on the diagonal and the entries neighboring the diagonal. We can then decompose it into a “kinetic” and a “potential” term. The kinetic part \hat{P}^{kin} is defined as the matrix with non-zero elements on the diagonal and in the neighboring entries, such that the sum of the elements in a row or a column is always zero. The potential part \hat{P}^{pot} is then the “left over” in the diagonal. Thus we have a tentative representation of \hat{P} as

$$\hat{P}_{ij} = \hat{P}_{ij}^{\text{kin}} + \hat{P}_{ij}^{\text{pot}}, \tag{20}$$

$$\hat{P}_{ij}^{\text{kin}} = p_i \Delta_{ij}, \quad \hat{P}_{ij}^{\text{pot}} = u_i \delta_{ij}, \tag{21}$$

where the matrices Δ_{ij} and δ_{ij} are defined above⁴. We know \hat{P} from the data, and we can make a least χ^2 -fit to determine the numbers p_i and u_i . For details we refer again to [3]. The results are shown in Fig. 10 and Fig. 11.

⁴ For subtleties in the definition of \hat{P}^{kin} and \hat{P}^{pot} related to the zero models we refer to [3].

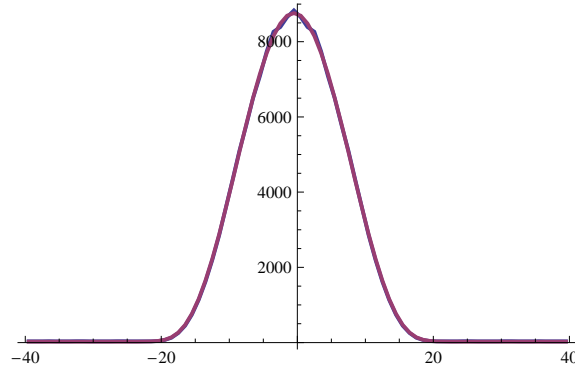


Fig. 10. The directly measured expectation values $\bar{N}_3(i)$ compared to the averages $\bar{N}_3(i)$ reconstructed from (22), for $\kappa_0 = 2.2$ and $\Delta = 0.6$.

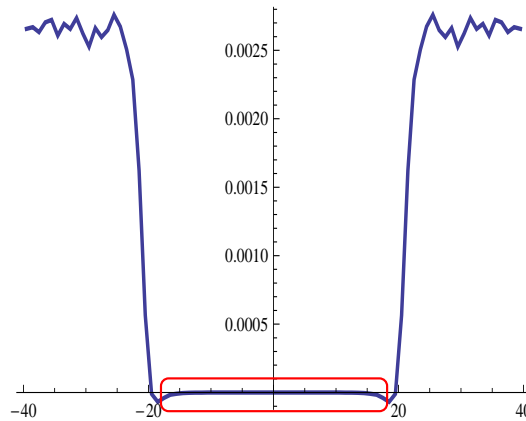


Fig. 11. Reconstructing the second derivative $U''(\bar{N}_3(i))$ from the coefficients u_i , for $\kappa_0 = 2.2$ and $\Delta = 0.6$ and $N_4^{(4,1)} = 160.000$.

Let us look at the discretized minisuperspace action (15) which obviously has served as an inspiration for the definitions of \hat{P}^{kin} and \hat{P}^{pot} . Expanding $N_3(i)$ to second order around $\bar{N}_3(i)$ one obtains the identifications

$$\bar{N}_3(i) = \frac{2k_1}{p_i}, \quad U''(\bar{N}_3(i)) = -u_i, \quad (22)$$

where $U(N_3(i)) = k_1 \tilde{k}_2 N_3^{1/3}(i)$ denotes the potential term in (15). We use the fitted coefficients p_i to reconstruct $\bar{N}_3(i)$ and then compare these reconstructed values with the averages $\bar{N}_3(i)$ measured directly. Similarly, we can use the measured u_i 's to reconstruct the second derivatives $U''(\bar{N}_3(i))$ and compare them to the form $\bar{N}_3^{-5/3}(i)$ coming from (15).

The reconstruction of $\bar{N}_3(i)$ is illustrated in Fig. 10 for a given four-volume N_4 and compared with the directly measured expectation values $\bar{N}_3(i)$. It is seen that the reconstruction works very well and, *most importantly*, the coupling constant k_1 , which in this way can be determined independently for each four-volume N_4 really *is* independent of N_4 in the range of N_4 's we have considered, as should be.

We will now try to extract the potential $U''(\bar{N}_3(i))$ from the information contained in the matrix \hat{P}^{pot} . The determination of $U''(\bar{N}_3(i))$ is not an easy task as can be understood from Fig. 11, which shows the measured coefficients u_i extracted from the matrix \hat{P}^{pot} , and which we consider somewhat remarkable. The interpolated curve makes an abrupt jump by two orders of magnitude going from the extended part of the universe (stretching over roughly 40 time steps) to the stalk. The occurrence of this jump is entirely dynamical, no distinction has ever been made by hand between stalk and bulk. In order to extract any physics information related to a genuine potential like the one appearing in (15) we have of course to restrict ourselves to the region of the “blob”, encircled in Fig. 11. It is clear that it is non-trivial to extract $U''(\bar{N}_3(i))$ from the data available in Fig. 11.

The range of the discrete three-volumes $N_3(i)$ in the extended universe is from several thousand down to five, the kinematically allowed minimum. However, the behavior for the very small values of $N_3(i)$ near the edge of the extended universe is likely to be mixed in with discretization effects. In order to test whether one really has a $N_3^{1/3}(i)$ -term in the action one should therefore only use values of $N_3(i)$ somewhat larger than five (shown as the encircled region in Fig. 11). This has been done in Fig. 12, where we have converted the coefficients u_i from functions of the discrete time steps i into functions of the background spatial three-volume $\bar{N}_3(i)$ using the identification in (22) (the conversion factor can be read off the relevant curve in Fig. 10). The data presented in Fig. 12 were taken at a discrete volume $N_4^{(4,1)} = 160.000$, and fit well the form $N_3^{-5/3}$, corresponding to a potential $\tilde{k}_2 N_3^{1/3}$.

Apart from obtaining the correct power $N_3^{-5/3}$ for the potential for a given spacetime volume N_4 , it is equally important that the coefficient in front of this term be independent of N_4 . This seems to be the case as is shown in Fig. 13, where we have plotted the measured potentials in terms of reduced, dimensionless variables which make the comparison between measurements for different N_4 's easier. In summary, we conclude that the data allow us to reconstruct the action (15) with good precision.

Let us emphasize a remarkable aspect of this result. Our starting point was the Regge action for CDT, as described in Sec. 2 above. However, the effective action we have generated dynamically by performing the nonper-

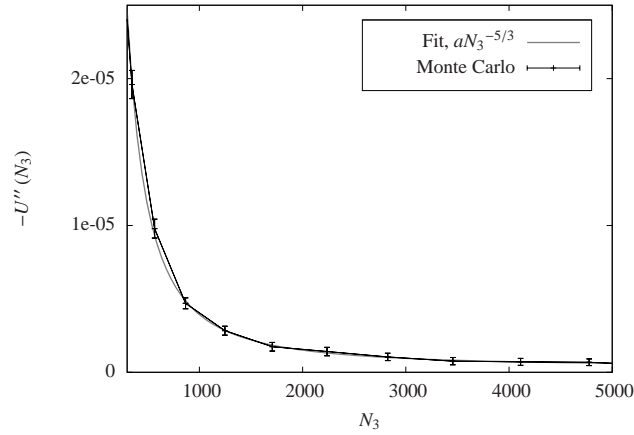


Fig. 12. The second derivative $-U''(N_3)$ as measured for $N_4^{(4,1)} = 160.000$ and $\kappa_0 = 2.2$ and $\Delta = 0.6$.

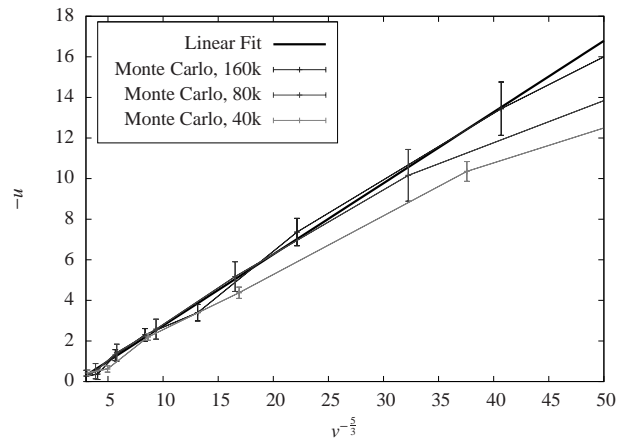


Fig. 13. The dimensionless second derivative $u = N_4^{5/4}U''(N_3)$ plotted against $\nu^{-5/3}$, where $\nu = N_3/N_4^{3/4}$ is the dimensionless spatial volume, for $N_4^{(4,1)} = 40.000$, 80.000 and 160.000, $\kappa_0 = 2.2$ and $\Delta = 0.6$. One expects a universal straight line near the origin (*i.e.* for large volumes) if the power law $U(N_3) \propto N^{1/3}$ is correct.

turbative sum over histories is only indirectly related to this “bare” action. Likewise, the coupling constant k_1 which appears in front of the effective action, and which we view as related to the gravitational coupling constant G by Eq. (16) has no obvious direct relation to the “bare” coupling κ_0 appearing in the Regge action (1) and in (4). Nevertheless the leading terms in the effective action for the scale factor are precisely the ones pre-

sented in (15). That a kinetic term with a second-order derivative appears as a leading term in an effective action is maybe less surprising, but it is remarkable and very encouraging for the entire CDT-quantization program that the kinetic term appears in precisely the correct combination with the factor $N_3(i)^{1/3}$ needed to identify the leading terms with the corresponding terms in the Einstein–Hilbert action. In other words, only if these terms are present can we claim to have an effective field theory which has anything to do with the standard diffeomorphism-invariant gravitational theory in the continuum. This is neither automatic nor obvious, since our starting point involved both a discretization and an explicit asymmetry between space and time, and since the nonperturbative interplay of the local geometric excitations we are summing over in the path integral is beyond our analytic control. Nevertheless, what we have found is that at least the leading terms in the effective action we have derived dynamically admit an interpretation as the standard Einstein term, thus passing a highly nontrivial consistency test.

5. Fluctuations around de Sitter space

In the following we will test in more detail how well the actions (14) and (15) describe the data encoded in the covariance matrix \hat{C} .

The correlation function was defined in the previous section by

$$C_{N_4}(i, i') = \langle \delta N_3(i) \delta N_3(i') \rangle, \quad \delta N_3(i) \equiv N_3(i) - \bar{N}_3(i), \quad (23)$$

where we have included an additional subscript N_4 to emphasize that N_4 is kept constant in a given simulation.

The first observation extracted from the Monte Carlo simulations is that under a change in the four-volume $C_{N_4}(i, i')$ scales as⁵

$$C_{N_4}(i, i') = N_4 F\left(i/N_4^{1/4}, i'/N_4^{1/4}\right), \quad (24)$$

where F is a universal scaling function. This is illustrated by Fig. 14 for the rescaled version of the diagonal part $C_{N_4}^{1/2}(i, i)$, corresponding precisely to the quantum fluctuations $\langle (\delta N_3(i))^2 \rangle^{1/2}$ of Fig. 5. While the height of the curve in Fig. 5 will grow as $N_4^{3/4}$, the superimposed fluctuations will only grow as $N_4^{1/2}$. We conclude that *for fixed bare coupling constants* the relative fluctuations will go to zero in the infinite-volume limit.

⁵ We stress again that the form (24) is only valid in that part of the universe whose spatial extension is considerably larger than the minimal S^3 constructed from 5 tetrahedra. (The spatial volume of the stalk typically fluctuates between 5 and 15 tetrahedra.)

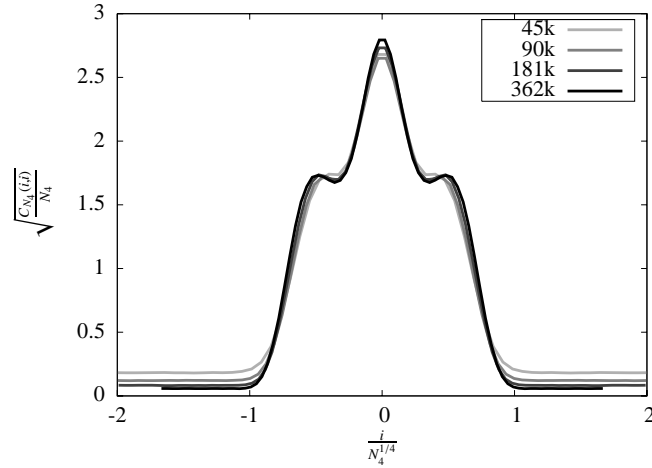


Fig. 14. Analyzing the quantum fluctuations of Fig. 5: diagonal entries $F(t, t)^{1/2}$ of the universal scaling function F from (24), for $N_4^{(4,1)} = 20.000, 40.000, 80.000$ and 160.000 .

Let us rewrite the minisuperspace action (14) for a fixed, finite four-volume V_4 in terms of dimensionless variables by introducing $s = t/V_4^{1/4}$ and $V_3(t) = V_4^{3/4}v_3(s)$:

$$S = \frac{1}{24\pi} \frac{\sqrt{V_4}}{G} \int ds \sqrt{g_{ss}} \left(\frac{g^{ss} \dot{v}_3^2(s)}{v_3(s)} + k_2 v_3^{1/3}(s) \right), \tag{25}$$

now assuming that $\int ds \sqrt{g_{ss}} v_3(s) = 1$, and with $g_{ss} \equiv g_{tt}$. The same rewriting can be done to (15) which becomes

$$S_{\text{discr}} = k_1 \sqrt{N_4} \sum_i \Delta s \left(\frac{1}{n_3(s_i)} \left(\frac{n_3(s_{i+1}) - n_3(s_i)}{\Delta s} \right)^2 + \tilde{k}_2 n_3^{1/3}(s_i) \right), \tag{26}$$

where $N_3(i) = N_4^{3/4} n_3(s_i)$ and $s_i = i/N_4^{1/4}$.

From the way the factor $\sqrt{N_4}$ appears as an overall scale in Eq. (26) it is clear that to the extent a quadratic expansion around the effective background geometry is valid one will have a scaling

$$\langle \delta N_3(i) \delta N_3(i') \rangle = N_4^{3/2} \langle \delta n_3(t_i) \delta n_3(t_{i'}) \rangle = N_4 F(t_i, t_{i'}), \tag{27}$$

where $t_i = i/N_4^{1/4}$. This implies that (24) provides additional evidence for the validity of the quadratic approximation and the fact that our choice of action (15), with k_1 independent of N_4 is indeed consistent.

To demonstrate in detail that the full function $F(t, t')$ and not only its diagonal part is described by the effective actions (14), (15), let us for convenience adopt a continuum language and compute its expected behavior. Expanding (14) around the classical solution according to $V_3(t) = V_3^{\text{cl}}(t) + x(t)$, the quadratic fluctuations are given by

$$\begin{aligned} \langle x(t)x(t') \rangle &= \int \mathcal{D}x(s) x(t)x(t') e^{-\frac{1}{2} \iint ds ds' x(s)M(s,s')x(s')} \\ &= M^{-1}(t, t'), \end{aligned} \tag{28}$$

where $\mathcal{D}x(s)$ is the normalized measure and the quadratic form $M(t, t')$ is determined by expanding the effective action S to second order in $x(t)$,

$$S(V_3) = S(V_3^{\text{cl}}) + \frac{1}{18\pi G} \frac{B}{V_4} \int dt x(t) \hat{H} x(t). \tag{29}$$

In expression (29), \hat{H} denotes the Hermitian operator

$$\hat{H} = -\frac{d}{dt} \frac{1}{\cos^3(t/B)} \frac{d}{dt} - \frac{4}{B^2 \cos^5(t/B)}, \tag{30}$$

which must be diagonalized under the constraint that $\int dt \sqrt{g_{tt}} x(t) = 0$, since V_4 is kept constant.

Let $e^{(n)}(t)$ be the eigenfunctions of the quadratic form given by (29) with the volume constraint enforced, ordered according to increasing eigenvalues λ_n . As we will discuss shortly, the lowest eigenvalue is $\lambda_1 = 0$, associated with translational invariance in time direction, and should be left out when we invert $M(t, t')$, because we precisely fix the centre of volume when making our measurements. Its dynamics is therefore not accounted for in the correlator $C(t, t')$.

If this cosmological continuum model were to give the correct description of the computer-generated universe, the matrix

$$M^{-1}(t, t') = \sum_{n=2}^{\infty} \frac{e^{(n)}(t)e^{(n)}(t')}{\lambda_n} \tag{31}$$

should be proportional to the measured correlator $C(t, t')$. Fig. 15 shows the eigenfunctions $e^{(2)}(t)$ and $e^{(4)}(t)$ (with two and four zeros, respectively), calculated from \hat{H} with the constraint $\int dt \sqrt{g_{tt}} x(t) = 0$ imposed. Simultaneously we show the corresponding eigenfunctions calculated from the data, *i.e.* from the matrix $C(t, t')$, which correspond to the (normalizable) eigenfunctions with the highest and third-highest eigenvalues. The agreement is

very good, in particular when taking into consideration that no parameter has been adjusted in the action (we simply take $B = s_0 N_4^{1/4} \Delta t$ in (11) and (29), which gives $B = 14.47 a_t$ for $N_4 = 362.000$).

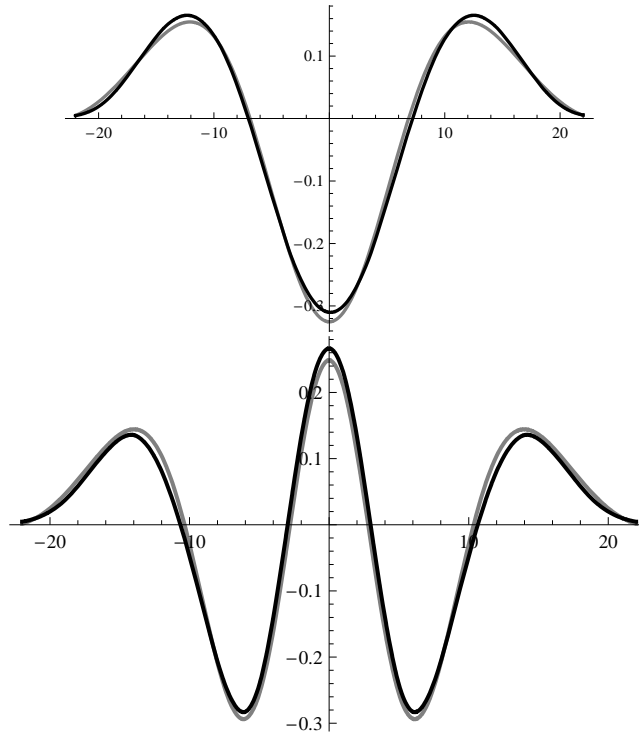


Fig. 15. Comparing the two highest even eigenvector of the covariance matrix $C(t, t')$ measured directly (gray curves) with the two lowest even eigenvectors of $M^{-1}(t, t')$, calculated semiclassically (black curves).

The reader may wonder why the first eigenfunction exhibited has two zeros. As one would expect, the ground state eigenfunction $e^{(0)}(t)$ of the Hamiltonian (30), corresponding to the lowest eigenvalue, has no zeros, but it does not satisfy the volume constraint $\int dt \sqrt{g_{tt}} x(t) = 0$. The eigenfunction $e^{(1)}(t)$ of \hat{H} with next-lowest eigenvalue has one zero and is given by the simple analytic function

$$e^{(1)}(t) = \frac{4}{\sqrt{\pi B}} \sin\left(\frac{t}{B}\right) \cos^2\left(\frac{t}{B}\right) = c^{-1} \frac{dV_3^{\text{cl}}(t)}{dt}, \quad (32)$$

where c is a constant. One realizes immediately that $e^{(1)}$ is the translational zero mode of the classical solution $V_3^{\text{cl}}(t)$ ($\propto \cos^3 t/B$). Since the action is invariant under time translations we have

$$S\left(V_3^{\text{cl}}(t + \Delta t)\right) = S\left(V_3^{\text{cl}}(t)\right), \tag{33}$$

and since $V_3^{\text{cl}}(t)$ is a solution to the classical equations of motion we find to second order (using the definition (32))

$$S\left(V_3^{\text{cl}}(t + \Delta t)\right) = S\left(V_3^{\text{cl}}(t)\right) + \frac{c^2(\Delta t)^2}{18\pi G} \frac{B}{V_4} \int dt e^{(1)}(t) \hat{H} e^{(1)}(t), \tag{34}$$

consistent with $e^{(1)}(t)$ having eigenvalue zero.

It is clear from Fig. 15 that some of the eigenfunctions of \hat{H} (with the volume constraint imposed) agree very well with the measured eigenfunctions. All even eigenfunctions (those symmetric with respect to reflection about the symmetry axis located at the centre of volume) turn out to agree very well. The odd eigenfunctions of \hat{H} agree less well with the eigenfunctions calculated from the measured $C(t, t')$. The reason seems to be that we have not managed to eliminate the motion of the centre of volume completely from our measurements. As already mentioned above, there is an inherent ambiguity in fixing the centre of volume, which turns out to be sufficient to reintroduce the zero mode in the data. Suppose we had by mistake misplaced the centre of volume by a small distance Δt . This would introduce a modification

$$\Delta V_3 = \frac{dV_3^{\text{cl}}(t)}{dt} \Delta t \tag{35}$$

proportional to the zero mode of the potential $V_3^{\text{cl}}(t)$. It follows that the zero mode can re-enter whenever we have an ambiguity in the position of the centre of volume. In fact, we have found that the first odd eigenfunction extracted from the data can be perfectly described by a linear combination of $e^{(1)}(t)$ and $e^{(3)}(t)$. It may be surprising at first that an ambiguity of one lattice spacing can introduce a significant mixing. However, if we translate ΔV_3 from Eq. (35) to “discretized” dimensionless units using $V_3(i) \sim N_4^{3/4} \cos(i/N_4^{1/4})$, we find that $\Delta V_3 \sim \sqrt{N_4}$, which because of $\langle (\delta N_3(i))^2 \rangle \sim N_4$ is of the same order of magnitude as the fluctuations themselves. In our case, this apparently does affect the odd eigenfunctions.

One can also compare the data and the matrix $M^{-1}(t, t')$ calculated from (31) directly. This is illustrated in Fig. 16, where we have restricted ourselves to data from inside the extended part of the universe. We imitate the construction (31) for M^{-1} , using the data to calculate the eigenfunctions, rather than \hat{H} . One could also have used $C(t, t')$ directly, but the use of the eigenfunctions makes it somewhat easier to perform the restriction to the bulk. The agreement is again good (better than 15% at any point on the plot), although less spectacular than in Fig. 15 because of the contribution of the odd eigenfunctions to the data.

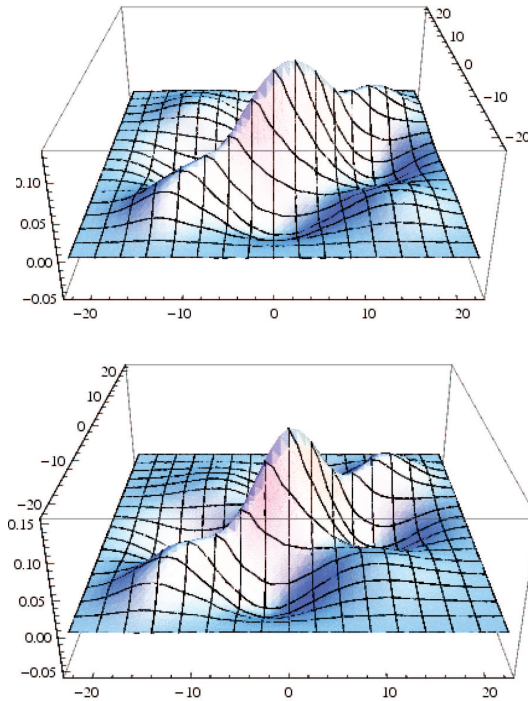


Fig. 16. Comparing data for the extended part of the universe: measured $C(t, t')$ (above) versus $M^{-1}(t, t')$ obtained from analytical calculation (below). The agreement is good, and would have been even better had we included only the even modes.

6. The size of the universe and the flow of G

It is natural to view the coupling constant G in front of the effective action for the scale factor as the gravitational coupling constant G . The effective action which described our computer generated data was given by Eq. (14) and its dimensionless lattice version by (15). The computer data allows us to extract $k_1 \propto a^2/G$, a being the spatial lattice spacing, the precise constant of proportionality being given by Eq. (16):

$$G = \frac{a^2 \sqrt{\tilde{C}_4} \tilde{s}_0^2}{k_1 3\sqrt{6}}. \quad (36)$$

For the bare coupling constants $(\kappa_0, \Delta) = (2.2, 0.6)$ we have high-statistics measurements for N_4 ranging from 45.500 to 362.000 four-simplices (equivalently, $N_4^{(4,1)}$ ranging from 20.000 to 160.000 four-simplices). The choice of Δ determines the asymmetry parameter α , and the choice of (κ_0, Δ) de-

termines the ratio ξ between $N_4^{(3,2)}$ and $N_4^{(4,1)}$. This in turn determines the “effective” four-volume \tilde{C}_4 of an average four-simplex, which also appears in (36). The number \tilde{s}_0 in (36) is determined directly from the time extension T_{univ} of the extended universe according to

$$T_{\text{univ}} = \pi \tilde{s}_0 \left(N_4^{(4,1)} \right)^{1/4}. \tag{37}$$

Finally, from our measurements we have determined $k_1 = 0.038$. Taking everything together according to (36), we obtain $G \approx 0.23a^2$, or $\ell_{\text{Pl}} \approx 0.48a$, where $\ell_{\text{Pl}} = \sqrt{G}$ is the Planck length.

From the identification of the volume of the four-sphere, $V_4 = 8\pi^2 R^4/3 = \tilde{C}_4 N_4^{(4,1)} a^4$, we obtain that $R = 3.1a$. In other words, *the linear size πR of the quantum de Sitter universes studied here lies in the range of 12-21 Planck lengths for N_4 in the range mentioned above and for the bare coupling constants chosen as $(\kappa_0, \Delta) = (2.2, 0.6)$.*

Our dynamically generated universes are therefore not very big, and the quantum fluctuations around their average shape are large as is apparent from Fig. 5. It is rather surprising that the semiclassical minisuperspace formulation is applicable for universes of such a small size, a fact that should be welcome news to anyone performing semiclassical calculations to describe the behavior of the early universe. However, in a certain sense our lattices are still coarse compared to the Planck scale ℓ_{Pl} because the Planck length is roughly half a lattice spacing. If we are after a theory of quantum gravity valid on all scales, we are in particular interested in uncovering phenomena associated with Planck-scale physics. In order to collect data free from unphysical short-distance lattice artifacts at this scale, we would ideally like to work with a lattice spacing much smaller than the Planck length, while still being able to set by hand the physical volume of the universe studied on the computer.

The way to achieve this, under the assumption that the coupling constant G of formula (36) is indeed a true measure of the gravitational coupling constant, is as follows. We are free to vary the discrete four-volume N_4 and the bare coupling constants (κ_0, Δ) of the Regge action (see [5] for further details on the latter). Assuming for the moment that the semiclassical minisuperspace action is valid, the effective coupling constant k_1 in front of it will be a function of the bare coupling constants (κ_0, Δ) , and can in principle be determined as described above for the case $(\kappa_0, \Delta) = (2.2, 0.6)$. If we adjusted the bare coupling constants such that in the limit as $N_4 \rightarrow \infty$ both

$$V_4 \sim N_4 a^4 \quad \text{and} \quad G \sim a^2/k_1(\kappa_0, \Delta) \tag{38}$$

remained constant (*i.e.* $k_1(\kappa_0, \Delta) \sim 1/\sqrt{N_4}$), we would eventually reach a region where the Planck length was significantly smaller than the lattice spacing a , in which event the lattice could be used to approximate spacetime structures of Planckian size and we could initiate a genuine study of the sub-Planckian regime. Since we have no control over the effective coupling constant k_1 , the first obvious question which arises is whether we can at all adjust the bare coupling constants in such a way that at large scales we still see a four-dimensional universe, with k_1 going to zero at the same time. The answer seems to be in the affirmative, as we will go on to explain. Fig. 17 shows the results of extracting k_1 for a range of bare coupling constants for which we still observe an extended universe. In the top figure $\Delta = 0.6$ is kept constant while κ_0 is varied. For κ_0 sufficiently large we eventually reach a point where a phase transition takes place (the point in the square in the bottom right-hand corner is the measurement closest to the transition we have looked at). For even larger values of κ_0 , beyond this transition, the universe disintegrates into a number of small universes, in a CDT-analogue of the branched-polymer phase of Euclidean quantum gravity. The plot shows that the effective coupling constant k_1 becomes smaller and possibly goes to zero as the phase transition point is approached, although our current data do not yet allow us to conclude that k_1 does indeed vanish at the transition point.

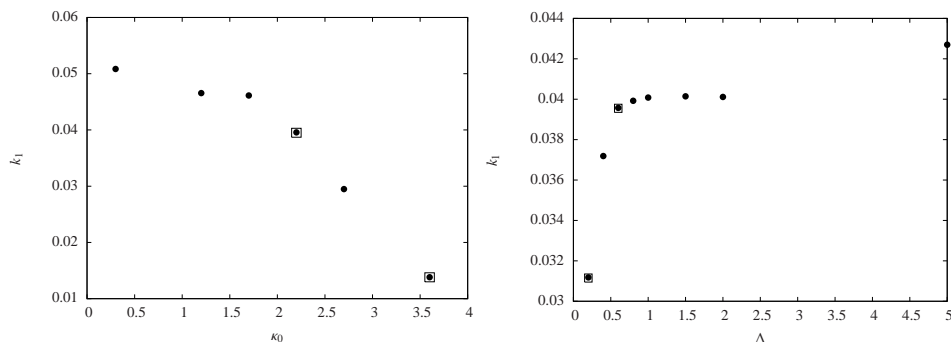


Fig. 17. The measured effective coupling constant k_1 as function of the bare κ_0 (top, $\Delta = 0.6$ fixed) and the asymmetry Δ (bottom, $\kappa_0 = 2.2$ fixed). The marked point near the middle of the data points sampled is the point $(\kappa_0, \Delta) = (2.2, 0.6)$ where most measurements in the remainder of the paper were taken. The other marked points are those closest to the two phase transitions, to the “branched-polymer phase” (top), and the “crumpled phase” (bottom).

Conversely, the bottom figure of Fig. 17 shows the effect of varying Δ , while keeping $\kappa_0 = 2.2$ fixed. As Δ is decreased towards 0, we eventually hit another phase transition, separating the physical phase of extended universes

from the CDT-equivalent of the crumpled phase of Euclidean quantum gravity, where the entire universe will be concentrated within a few time steps, as already mentioned in Sec. 3 above. (The point closest to the transition where we have taken measurements is the one in the bottom left-hand corner.) Also when approaching this phase transition the effective coupling constant k_1 goes to 0, leading to the tentative conclusion that $k_1 \rightarrow 0$ along the entire phase boundary.

However, to extract the coupling constant G from (36) we not only have to take into account the change in k_1 , but also that in \tilde{s}_0 (the width of the distribution $N_3(i)$) and in the effective four-volume \tilde{C}_4 as a function of the bare coupling constants. Combining these changes, we arrive at a slightly different picture. Approaching the boundary where spacetime collapses in time direction (by lowering Δ), the gravitational coupling constant G *decreases*, despite the fact that $1/k_1$ increases. This is a consequence of \tilde{s}_0 decreasing considerably, as can be seen from Fig. 8. On the other hand, when (by increasing κ_0) we approach the region where the universe breaks up into several independent components, the effective gravitational coupling constant G increases, more or less like $1/k_1$, where the behavior of k_1 is shown in Fig. 17 (top). This implies that the Planck length $\ell_{\text{Pl}} = \sqrt{G}$ increases from approximately $0.48a$ to $0.83a$ when κ_0 changes from 2.2 to 3.6. Most likely we can make it even bigger in terms of Planck units by moving closer to the phase boundary.

On the basis of these arguments, it seems likely that the nonperturbative CDT-formulation of quantum gravity does allow us to penetrate into the sub-Planckian regime and probe the physics there explicitly. Work in this direction is currently ongoing. One interesting issue under investigation is whether and to what extent the simple minisuperspace description remains valid as we go to shorter scales. We have already seen deviations from classicality at short scales when measuring the spectral dimension [5, 21], and one would expect them to be related to additional terms in the effective action (14) and/or a nontrivial scaling behavior of k_1 . This raises the interesting possibility of being able to test explicitly the scaling violations of G predicted by renormalization group methods in the context of asymptotic safety [2].

7. Discussion

Let us summarize the assumption used in our regularized model, the results obtained and then discuss the possible implications.

The CDT model of quantum gravity is extremely simple. It is the path integral over the class of causal geometries with a global time foliation. In order to perform the summation explicitly, we introduce a grid of piecewise

linear geometries, much in the same way as when defining the path integral in quantum mechanics. Next, we rotate each of these geometries to Euclidean signature and use as bare action the Einstein–Hilbert action⁶ in Regge form. That is all.

The resulting superposition exhibits a nontrivial scaling behavior as function of the four-volume, and we observe the appearance of a well-defined average geometry, that of de Sitter space, the maximally symmetric solution to the classical Einstein equations in the presence of a positive cosmological constant. We are definitely in a quantum regime, since the fluctuations of the three-volume around de Sitter space are sizable, as can be seen in Fig. 5. Both the average geometry and the quantum fluctuations are well described in terms of the minisuperspace action (14). A key feature to appreciate is that, unlike in standard (quantum-)cosmological treatments, this description is the *outcome* of a nonperturbative evaluation of the *full* path integral, with everything but the scale factor (equivalently, $V_3(t)$) summed over. Measuring the correlations of the quantum fluctuations in the computer simulations for a particular choice of bare coupling constants enabled us to determine the continuum gravitational coupling constant G as $G \approx 0.42a^2$, thereby introducing an absolute physical length scale into the dimensionless lattice setting. Within measuring accuracy, our de Sitter universes (with volumes lying in the range of 6.000–47.000 ℓ_{Pl}^4) are seen to behave perfectly semiclassically with regard to their large-scale properties.

We have also indicated how we may be able to penetrate into the sub-Planckian regime by suitably changing the bare coupling constants. By “sub-Planckian regim” we mean that the lattice spacing a is (much) smaller than the Planck length. While we have not yet analyzed this region in detail, we expect to eventually observe a breakdown of the semiclassical approximation. This will hopefully allow us to make contact with attempts to use renormalization group techniques in the continuum and the concept of asymptotic safety to study scaling violations in quantum gravity [2].

On the basis of the results presented here, two major issues suggest themselves for further research. First, we need to establish the relation of our effective gravitational coupling constant G with a more conventional gravitational coupling constant, defined directly in terms of coupling matter to gravity. In the present work, we have defined G as the coupling constant in front of the effective action, but it would be desirable to verify directly that a gravitational coupling defined via the coupling to matter agrees with our G . In principle it is easy to couple matter to our model, but it is less straightforward to define in a simple way a set-up for extracting the semiclassical effect of gravity on the matter sector. Attempts in this direction

⁶ Of course, the full, effective action, including measure contributions, will contain all higher-derivative terms.

were already undertaken in the “old” Euclidean approach [23, 24], and it is possible that similar ideas can be used in CDT quantum gravity. Work on this is in progress.

The second issue concerns the precise nature of the “continuum limit”. In a conventional lattice-theoretic setting the continuum limit is usually linked to a divergent correlation length at a critical point. It is unclear whether such a scenario is realized in our case. In general, it is rather unclear how one could define at all the concept of a divergent length related to correlators in quantum gravity, since one is integrating over all geometries, and it is the geometries which dynamically give rise to the notion of “length”, as already discussed in the introduction.

This has been studied in detail in two-dimensional (Euclidean) quantum gravity coupled to matter with central charge $c \leq 1$ [25]. It led to the conclusion that one could associate the critical behavior of the matter fields (*i.e.* approaching the critical point of the Ising model) with a divergent correlation length, although the matter correlators themselves had to be defined as non-local objects due to the requirement of diffeomorphism invariance. On the other hand, the two-dimensional studies do not give us a clue of how to treat the gravitational sector itself, since they do not possess gravitational field-theoretic degrees of freedom. What happens in the two-dimensional lattice models which can be solved analytically is that the only fine-tuning needed to approach the continuum limit is an additive renormalization of the cosmological constant (for fixed matter couplings). Thus, fixing the two-dimensional spacetime volume N_2 (the number of triangles), such that the cosmological constant plays no role, there are no further coupling constants to adjust and the continuum limit is automatically obtained by the assignment $V_2 = N_2 a^2$ and taking $N_2 \rightarrow \infty$. This situation can also occur in special circumstances in ordinary lattice field theory. A term like

$$\sum_i c_1(\phi_{i+1} - \phi_i)^2 + c_2(\phi_{i+1} + \phi_{i-1} - 2\phi_i)^2 \quad (39)$$

(or a higher-dimensional generalization) will also go to the continuum free field theory simply by increasing the lattice size and using the identification $V_d = L^d a^d$ (L denoting the linear size of the lattice in lattice units), the higher-derivative term being sub-dominant in the limit. It is not obvious that in quantum gravity one can obtain a continuum quantum field theory without fine-tuning in a similar way, because the action in this case is multiplied by a dimensionful coupling constant. Nevertheless, it is certainly remarkable that the infrared limit of our effective action apparently reproduces — within the cosmological setting — the Einstein–Hilbert action, which is the unique diffeomorphism-invariant generalization of the ordinary kinetic term, containing at most second derivatives of the metric. A major ques-

tion is whether and how far our theory can be pushed towards an ultraviolet limit. We have indicated how to obtain such a limit by varying the bare coupling constants of the theory, but the investigation of the limit $a \rightarrow 0$ with fixed G has only just begun. Another possibility is that spacetime effectively ceases to exist as a relevant concept when we reach the Planck scale. The correct field theory at such short distances could be a topological field theory where one effectively has $\langle g_{\mu\nu}(x) \rangle = 0$. This is an old idea, but no real implementation of a transition from a phase where a background geometry exists to a phase where $\langle g_{\mu\nu}(x) \rangle = 0$ has ever been given. If such a scenario is correct it is unlikely that one can penetrate into the sub-Planckian regime in the lattice simulations. Thus it becomes important to understand how we can distinguish between the situation where there is no sensible UV limit in our model and the situation where the impossibility to penetrate into sub-Planckian regime signals interesting physics. Work in this direction is in progress.

All authors acknowledge support by ENRAGE (European Network on Random Geometry), a Marie Curie Research Training Network, contract MRTN-CT-2004-005616, and A.G. and J.J. by COCOS (Correlations in Complex Systems), a Marie Curie Transfer of Knowledge Project, contract MTKD-CT-2004-517186, both in the European Community's Sixth Framework Programme. R.L. acknowledges support by the Netherlands Organisation for Scientific Research (NWO) under their VICI program.

REFERENCES

- [1] S. Weinberg, *Ultraviolet Divergences in Quantum Theories of Gravitation*, in *General Relativity: Einstein Centenary Survey*, eds. S.W. Hawking, W. Israel, Cambridge University Press, Cambridge, UK, 1979, pp. 790–831.
- [2] A. Codello, R. Percacci, C. Rahmede, 0805.2909 [hep-th](#); M. Reuter, F. Saueressig, 0708.1317 [hep-th](#); M. Niedermaier, M. Reuter, *Living Rev. Rel.* **9**, 5 (2006); H.W. Hamber, R.M. Williams, *Phys. Rev.* **D72**, 044026 (2005) [[hep-th/0507017](#)]; D.F. Litim, *Phys. Rev. Lett.* **92**, 201301 (2004) [[hep-th/0312114](#)]; H. Kawai, Y. Kitazawa, M. Ninomiya, *Nucl. Phys.* **B467**, 313 (1996) [[hep-th/9511217](#)].
- [3] J. Ambjorn, A. Gorlich, J. Jurkiewicz, R. Loll, *Phys. Rev.* **D78**, 063544 (2008) [[arXiv:0807.4481](#) [[hep-th](#)]].
- [4] J. Ambjorn, J. Jurkiewicz, R. Loll, *Nucl. Phys.* **B610**, 347 (2001) [[hep-th/0105267](#)].
- [5] J. Ambjorn, J. Jurkiewicz, R. Loll, *Phys. Rev.* **D72**, 064014 (2005) [[hep-th/0505154](#)].
- [6] J. Ambjorn, R. Loll, *Nucl. Phys.* **B536**, 407 (1998) [[hep-th/9805108](#)].

- [7] J. Ambjørn, J. Jurkiewicz, R. Loll, *Phys. Rev. Lett.* **93**, 131301 (2004) [hep-th/0404156].
- [8] J. Ambjørn, J. Jurkiewicz, R. Loll, *Phys. Lett.* **B607**, 205 (2005) [hep-th/0411152].
- [9] J. Ambjørn, A. Görlich, J. Jurkiewicz, R. Loll, *Phys. Rev. Lett.* **100**, 091304 (2008) [0712.2485 hep-th].
- [10] J. Ambjørn, J. Jurkiewicz, R. Loll, [0806.0397 gr-qc].
- [11] J. Ambjørn, J. Jurkiewicz, R. Loll, *Contemp. Phys.* **47**, 103 (2006) [hep-th/0509010]; R. Loll, *Class. Quant. Grav.* **25**, 114006 (2008) [0711.0273 gr-qc].
- [12] C. Teitelboim, *Phys. Rev. Lett.* **50**, 705 (1983); *Phys. Rev.* **D28**, 297 (1983).
- [13] J. Ambjørn, R. Loll, W. Westra, S. Zohren, *J. High Energy Phys.* **0712**, 017 (2007) [0709.2784 gr-qc]; J. Ambjørn, R. Loll, Y. Watabiki, W. Westra, S. Zohren, *J. High Energy Phys.* **0805**, 032 (2008) [0802.0719 hep-th]; *Phys. Lett.* **B665**, 252 (2008) [0804.0252 hep-th]; arXiv:0810.2408 [hep-th]; arXiv:0810.2503 [hep-th].
- [14] J. Ambjørn, J. Jurkiewicz, R. Loll, G. Vernizzi, *J. High Energy Phys.* **0109**, 022 (2001) [hep-th/0106082]; *Acta Phys. Pol. B* **34**, 4667 (2003) [hep-th/0311072]; J. Ambjørn, J. Jurkiewicz, R. Loll, *Phys. Lett.* **B581**, 255 (2004) [hep-th/0307263].
- [15] D. Benedetti, R. Loll, F. Zamponi, *Phys. Rev.* **D76**, 104022 (2007) [0704.3214 hep-th].
- [16] J. Ambjørn, B. Durhuus, J. Fröhlich, *Nucl. Phys.* **B257**, 433 (1985); J. Ambjørn, B. Durhuus, J. Fröhlich, P. Orland, *Nucl. Phys.* **B270**, 457 (1986).
- [17] A. Billoire, F. David, *Phys. Lett.* **B168**, 279 (1986).
- [18] D.V. Boulatov, V.A. Kazakov, I.K. Kostov, A.A. Migdal, *Nucl. Phys.* **B275**, 641 (1986).
- [19] J. Ambjørn, J. Jurkiewicz, *Phys. Lett.* **B278**, 42 (1992).
- [20] M.E. Agishtein, A.A. Migdal, *Mod. Phys. Lett.* **A7**, 1039 (1992).
- [21] J. Ambjørn, J. Jurkiewicz, R. Loll, *Phys. Rev. Lett.* **95**, 171301 (2005) [hep-th/0505113].
- [22] B. Dittrich, R. Loll, *Class. Quantum Grav.* **23**, 3849 (2006) [gr-qc/0506035].
- [23] B.V. de Bakker, J. Smit, *Nucl. Phys.* **B484**, 476 (1997) [hep-lat/9604023].
- [24] H.W. Hamber, R.M. Williams, *Nucl. Phys.* **B435**, 361 (1995) [hep-th/9406163].
- [25] J. Ambjørn, K.N. Anagnostopoulos, U. Magnea, G. Thorleifsson, *Phys. Lett.* **B388**, 713 (1996) [hep-lat/9606012]; J. Ambjørn, K.N. Anagnostopoulos, *Nucl. Phys.* **B497**, 445 (1997) [hep-lat/9701006]; J. Ambjørn, K. N. Anagnostopoulos, R. Loll, *Phys. Rev.* **D60**, 104035 (1999) [hep-th/9904012].
- [26] J. Ambjørn, S. Jain, J. Jurkiewicz, C.F. Kristjansen, *Phys. Lett.* **B305**, 208 (1993) [hep-th/9303041].
- [27] J. Ambjørn, S. Jain, G. Thorleifsson, *Phys. Lett.* **B307**, 34 (1993) [hep-th/9303149].